

Crystallization-Induced Shrinkage, Crystalline, and Thermomechanical Properties of *In Situ* Polymerized Cyclic Butylene Terephthalate

M. Harsch,¹ J. Karger-Kocsis,² A. A. Apostolov³

¹Robert Bosch GmbH, Robert-Bosch-Straße, D-87542 Blaichach, Germany

²Institut für Verbundwerkstoffe GmbH, Kaiserslautern University of Technology, D-67663 Kaiserslautern, Germany

³Laboratory on Structure and Properties of Polymers, Faculty of Chemistry, Sofia University, BG-1164 Sofia, Bulgaria

Received 29 May 2007; accepted 1 December 2007

DOI 10.1002/app.27798

Published online 23 January 2008 in Wiley InterScience (www.interscience.wiley.com).

ABSTRACT: The polymerization and crystallization of cyclic butylene terephthalate oligomers (CBT) were followed by fiber Bragg grating (FBG) and normal force measurements under isothermal conditions at $T = 170$ and 190°C , respectively. It was found that the FBG and normal force sense only the crystallization-induced shrinkage. The course of the FBG signal and the normal force as a function of time suggested that crystallization of the polymerized CBT (pCBT) occurs in two steps. The primary crystallization-induced shrinkage is several hundreds by contrast to the secondary one showing several tens in ppm/min unit according to the FBG results. The two-step crystallization was confirmed by normal force measurements. The crystallinity and crystalline structure of the pCBTs were

studied by differential scanning calorimetry and wide-angle X-ray scattering. It was found that the crystallinity and the crystalline parameters slightly differ for the pCBTs formed at $T = 170$ and 190°C , respectively. The pCBT produced at $T = 190^\circ\text{C}$ had slightly higher crystallinity and more perfect crystals than the pCBT formed at $T = 170^\circ\text{C}$. The reliability of the FBG sensing was checked by thermomechanical analysis (TMA). A fair agreement was established between the thermal contraction and thermal expansion measured by FBG and TMA, respectively. © 2008 Wiley Periodicals, Inc. *J Appl Polym Sci* 108: 1455–1461, 2008

Key words: thermal properties; crystallization; polyesters; ring-opening polymerization; CBT oligomer

INTRODUCTION

Numerous cyclic monomers and oligomers can be converted into the related linear polymers. Researchers were always fascinated by this technique providing many advantages with respect to processing with and without additional reinforcements (low initial melt viscosity, good wet-out of reinforcements). This is the driving force nowadays to synthesize macrocyclic oligomers (oligomeric “precursors”) for high-temperature resistant thermoplastics including poly(aryl-ether ketones) and poly(phenylenes sulphides), as well as those in Refs. 1 and 2; and references therein.

Cyclic butylene terephthalate (CBT) oligomers are now available commercially. The related CBT products of Cyclics (www.cyclics.com) became under spot of vivid scientific and technical interests. The reason for the academic interest is mostly due to peculiarities in the crystalline structure of the result-

ing poly(butylene terephthalate) (pCBT) and copolymerization possibilities of CBT with other cyclics and their polymers.^{3,4} On the other hand, the industrial interest is directed to exploit the low viscosity of the CBT (tens of mPas).^{5–8} Note that the productivity of the related liquid composite molding process is comparable with that of the resin transfer molding of thermosets. Interestingly, the polymerization of CBT can be performed also below the melting temperature of pCBT ($=225^\circ\text{C}$). The industry prefers the isothermal polymerization of CBT at $T = 170$ – 195°C . This is because the polymerization is accompanied by crystallization, and thus the solidified (crystallized) product can be removed from the mold without subsequent cooling of the mold. Modulated and traditional differential scanning calorimetric (MDSC and DSC, respectively) studies indicated that the crystallization of the polymerized CBT strongly depends on the thermal conditions (kinetic factors).^{8–10} Moreover, the resulting crystalline structure has also some special features. pCBT has higher crystallinity and more perfect crystals than traditionally produced poly(butylene terephthalate) (PBT).⁴

From technological point of view it is of paramount importance to understand and control the crystallization of the *in situ* polymerized CBT. Recall that crystallization is accompanied with considerable

Correspondence to: J. Karger-Kocsis (karger@ivw.uni-kl.de).

Contract grant sponsor: DFG; contract grant number: Ka 1202/19.

Contract grant sponsor: BMBF (Pro-PBT).

volume shrinkage. This has to be “compensated” by changing the processing parameters during molding to produce void-free parts.⁸ The first task in this respect is, however, to detect the polymerization and crystallization-induced shrinkage accordingly. Chemical and physical changes, associated with stress/strain developments in polymers can adequately be followed by various techniques. Fiber Bragg grating sensing (FBG) is a rather new method to detect the strain build-up. FBG was already successfully used to study the cure-induced strain development in thermosets and thus to determine the optimum curing cycle.^{11–13} It is noteworthy, that the FBG technique is far more established for health monitoring of composite parts in which strain changes are caused by different failure events (e.g., Ref. 14). Another method to get information on the stress build-up is the measurement of the normal force during the *in situ* polymerization of CBT using a suitable rheometer.

To adopt the above techniques, the polymerization and crystallization of CBT is a very promising approach to shed light on the following open questions: (i) whether strain build-up occurs owing to polymerization, (ii) whether polymerization and crystallization run parallel or consecutively, and (iii) how the processing temperature affects the crystallization behavior.

Accordingly, this work was devoted to study the polymerization and crystallization behaviors of *in situ* polymerized CBT at various temperatures ($T = 170$ and 190°C , respectively) using the FBG and normal force measurement techniques. The resulting pCBT was object of wide-angle X-ray scattering (WAXS), DSC, and thermomechanical analysis (TMA) studies.

EXPERIMENTAL

Material

CBT powder (Grade:XB3-CA4) purchased from Cyclics (Schenectady, NY; www.cyclics.com) was used throughout this study. This CBT already contains the polymerization catalyst and thus termed as one-component CBT. CBT was dried in a vacuum oven for about 12 h at 85°C and was kept in a desiccator until further use.

Testing

FBG measurements

The CBT powder, preheated at $T = 85^\circ\text{C}$, was placed in a cylindrical aluminium mould (sample holder). The mold, containing a vertically placed FBG sensor, was covered from its inner side by poly(tetrafluoroethylene) (PTFE) film (thickness less than 0.1 mm)

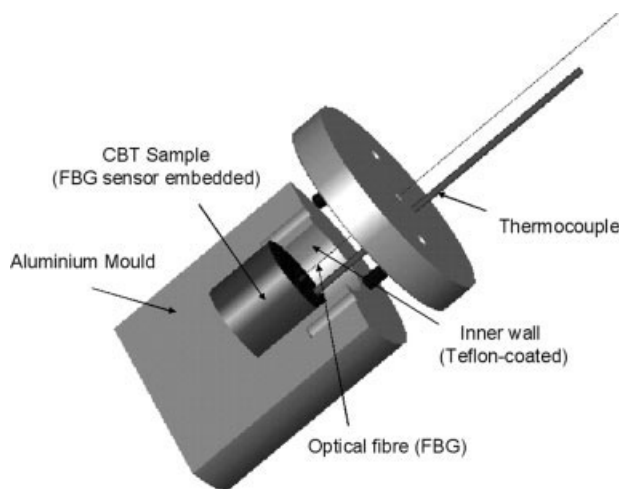


Figure 1 Experimental setup of the FBG measurement. Note: during the test the aluminium mold is positioned vertically.

and kept at the selected testing temperature (i.e., $T = 170$ and 190°C , respectively). Covering the cavity with PTFE was foreseen not to influence the CBT polymerization and crystallization, and especially to allow the free shrinkage of the pCBT during crystallization. The FBG sensor was aligned along the center axis of the cylindrical mold cavity (cf. Fig. 1). The CBT powder was introduced in the cavity of the mold and placed in a thermostatic oven. The oven was programmed for the temperature ramp: isothermal holding for 4 h at $T = 170$ or 190°C , followed by cooling to ambient temperature with $1^\circ\text{C}/\text{min}$. The experimental setup for the FBG measurement is given by Figure 1, and a detailed scheme of the FBG sensor is displayed in Figure 2. The FBG is a segment of the optical fiber with a periodic modulation of the core refractive index, which makes use of the Bragg reflectivity to detect axial changes along the optical fiber. A broad spectrum incident light with a central wavelength of 1549 nm was guided along the glass fiber. The back-reflected wavelength from the Bragg Gratings (Corning SMF28) was detected by an optical spectrum analyzer (AWE-CCD-1550, AOS GmbH, Dresden, Germany) and transmitted to a data evaluation processor unit. Strain and/or temperature changes affect the effective refractive index or the periodic spacing, and thereby entail a shift in the Bragg grating wavelength. This shift can be detected by the optical spectrum analyzer with an accuracy of 1 ppm. To consider the influence of temperature on the strain signal, the actual temperature was measured by a thermocouple in the sample next to the FBG sensor. The thermal contribution to the detected strain signal was eliminated so that the strain values, given later, are all linked with the “real” dimensional change due to the CBT polymer-

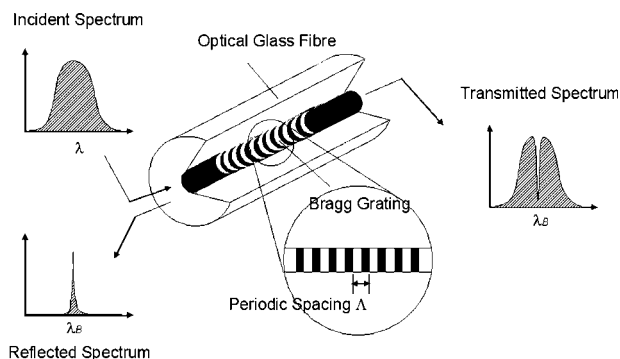


Figure 2 Principle of the FBG sensing technique.

ization/crystallization. Further information about the theoretical background of the FBG theory as well as the measuring setup of the Bragg wavelength shift, is disclosed in the literature.¹⁵

Normal force measurements

Development of the normal force was measured in a rheometer MARS (Thermo, Karlsruhe, Germany) equipped with a Peltier heating unit TCP/P. The CBT powder was placed into the preheated device and polymerized between two static parallel plates with a diameter of 60 mm and a constant gap of 0.5 mm. Temperature was set for $T = 170$ and 190°C , respectively, and the measurement lasted for 120 min. Normal force induced by the polymerizing/crystallizing CBT was measured in direction perpendicular to the plates by keeping the gap distance constant.

DSC

DSC was performed on DSC 821 device of Mettler Toledo (Giessen, Germany) calibrated with indium. Experiments were run with samples ranging from 8 to 10 mg under nitrogen to prevent moisture and oxidative degradation. The CBT samples were subjected to isothermal treatment at $T = 170$ and 190°C , respectively, for ca. 150 min.

WAXS investigations

A D500 X-ray diffractometer from Siemens (München, Germany) was used for recording the WAXS spectra of the pCBTs produced. Copper anode in conjunction with a secondary beam monochromator to separate K_α radiation was used. The scans were made in 2θ range from 5° to 60° . The apparent crystallite size in three directions was calculated from the full width at half height (FWHH) of the corresponding diffraction peaks using the well-known Scherrer's formula.

TMA

The linear thermal expansion of the pCBTs after the FBG tests was determined in a TMA 40 device (Mettler Toledo, Giessen, Germany) at a heating rate of $1^\circ\text{C}/\text{min}$ in the temperature range from ambient to 200°C at a minimum contact pressure.

It is noteworthy that our goal with the WAXS, DSC, and TMA tests was to elucidate whether the pCBTs produced in the FBG tests at $T = 170$ and 190°C , respectively, are identical or not.

RESULTS AND DISCUSSION

Figure 3 shows the FBG strain versus time (t) and temperature (T) versus time curves monitored during the test performed at $T = 190^\circ\text{C}$. Considering the $T-t$ curve one can see that the set temperature, viz., $T = 190^\circ\text{C}$, was reached at $t \approx 50$ min. On the other hand, the cooling rate was very close to the selected one ($1^\circ\text{C}/\text{min}$). The course of the FBG signal as a function of time is quite complex. The initial slight strain increase is likely linked to the melting of the CBT powder. No FBG signal change can be noticed for the following section (horizontal run), although the polymerization of the CBT should have been already completed. Note that rheological tests in parallel plate configuration demonstrated that the polymerization time for this CBT at $T = 190^\circ\text{C}$ is ca. 12 min.⁷ By contrast to curing thermosets,^{11–13} FBG sensing does not help us to detect a gel-like stage defined by $G' = G''$, where G' and G'' denote the storage and loss shear moduli, respectively. This can be considered, however, as a strong support that the ring-opening polymerization of CBT is entropy-driven, indeed. So, the transformation of the macrocyclic compounds to a linear polymer happens without any steric

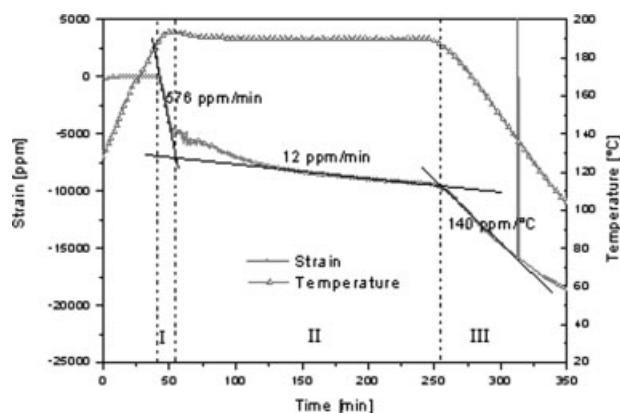


Figure 3 Strain development in the CBT hold at 190°C for 240 min. Note: this figure contains the estimated linear strain rate (in ppm/min unit) and thermal contraction (in ppm/ $^\circ\text{C}$ unit) data for the different time intervals.

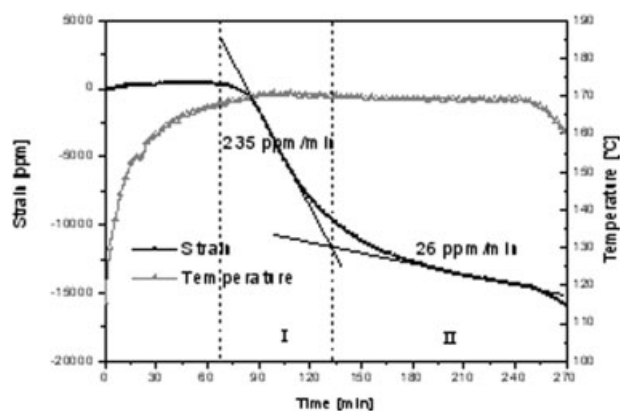


Figure 4 Strain development in the CBT hold at 170°C for 240 min. For note cf. Figure 3.

hindrance that would be accompanied with strain build-up. Recall that based on rheological tests the polymerization was likely completed, or at least highly advanced, before a sudden drop in the FBG strain occurred (see section I). Accordingly, this steep change in the FBG signal can be assigned to the crystallization. It is noteworthy that the rapid crystallization starts just before $T = 190^{\circ}\text{C}$ was reached (cf. section I in Fig. 3). The crystallization probably occurs in two steps. The primary crystallization is very fast causing a shrinkage rate of ca. 576 ppm/min. The secondary crystallization in section II is a slower procedure giving a shrinkage rate of ca. 12 ppm/min (when considering the marked linear approximations in Fig. 3). Section III in Figure 3 is caused by the cooling, and thus represents the thermal contraction of pCBT. Its value can be given by ca. 140 ppm/°C. Note that we should obtain a very similar value in the TMA test upon heating of the related pCBT. If this will be the case then we have an independent proof for the reliability of the FBG sensing. Reliability implies at the same time that the FBG sensor was well adhered to the pCBT formed.

Performing the FBG sensing during the *in situ* polymerization of CBT at $T = 170^{\circ}\text{C}$ (cf. Fig. 4) a similar scenario, as noticed for $T = 190^{\circ}\text{C}$, can be found. On the other hand, the crystallization-induced contractions in sections I and II differ substantially from those recorded at $T = 190^{\circ}\text{C}$. Before starting with the discussion, it has to be emphasized that the polymerization time of this CBT at $T = 170^{\circ}\text{C}$ is ca. 20 min.⁷ So, again the CBT is likely fully polymerized at $t \approx 70$ min, i.e., prior to the onset of the crystallization. This is a very important and new finding. It is often claimed in the literature that polymerization and crystallization take place simultaneously under isothermal conditions below the melting temperature of the resulting PBT.⁴ This is likely not the case here. Anyway, the crystallization-caused contraction rates

in the sections I and II are ca. 235 and 26 ppm/min, respectively (cf. Fig. 4). The slow-down of the primary crystallization at lower temperature is according to the expectation as the crystallization rate should also be slower at lower temperatures. However, the secondary crystallization in section II is faster than at $T = 190^{\circ}\text{C}$.

Further insight in the crystallization process was expected from the normal force measurements. Figure 5 shows the course of the normal force (negative sign indicate tensile force) versus time for the *in situ* polymerizing CBT at $T = 170$ and 190°C , respectively. By contrast to FBG test, the CBT placed between the two aluminum disks of the rheometer did not experience a lag in respect to the set temperature. This is the reason why the temperature–time traces are not indicated in Figure 5. Substantial deviation from the initial horizontal section of the normal force occurs at ca. 12 and 17 min at $T = 170$ and 190°C , respectively. At this time the polymerization should have been highly advanced, or even completed, based on rheological test results.⁷ Accordingly, the linearly decreasing normal force can be attributed again to the crystallization. The normal force versus time traces can be approximated by two linear sections before reaching some kind of plateau—cf. the related lines in Figure 5. This is in accord with the finding from FBG and thus represents a further proof for the supposed two-step crystallization.

The contraction rate (in ppm/min unit) and load development rate (in N/min unit) in section I and II (fast and slow crystallization, respectively) can be used to estimate the activation energy of the crystallization steps. By adopting the Arrhenius equation for these rates (β) in sections I and II at $T = 170$ and

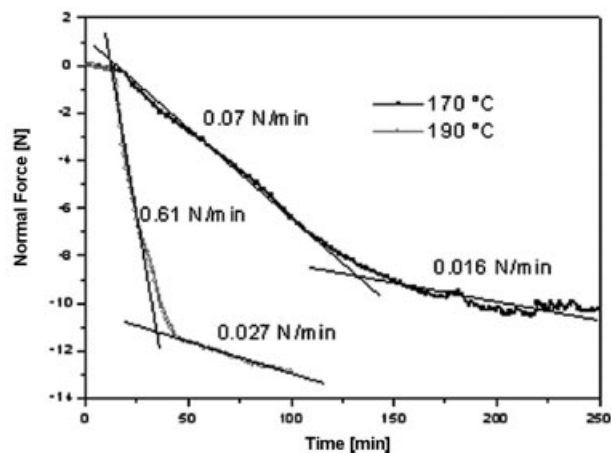


Figure 5 Normal force development in the CBT hold at $T = 170$ and 190°C , respectively. Note: this figure contains the estimated normal force rate (in N/min unit) data for the different crystallization stages (I and II).

190°C the related activation energies can be estimated by:

$$\beta = A \cdot \exp\left(-\frac{E_A}{RT}\right)$$

$$\ln \beta = \ln A - \frac{E_A}{R} \cdot \frac{1}{T}$$

where A is the preexponential constant, E_A is the activation energy of crystallization, R is the universal gas constant, and T is the absolute temperature. Because of uncertainties in the rate values in section II, E_A has been derived only for section I, i.e., fast crystallization. For the related activation energy values ca. 80 and 150 kJ/mol were found from the FBG and normal force measurements, respectively. The activation energies scatter in a very broad range. It should be born in mind that these activation energies are very rough estimates due to the following: only two temperatures were taken into account, results derived from one (FBG) and two (normal force) tests, and the rate functions considered have been already approximated.

Nevertheless, these values are markedly lower than the activation energy of pCBT crystallized from the melt. When the same pCBT was cooled from the melt (starting at $T = 250^\circ\text{C}$) at various cooling rates, activation energies of 150 and 360 kJ/mol were concluded. The above two values are linked with two sections of the corresponding Kissinger plots. By contrast, traditional PBT exhibited a crystallization activation energy of ca. 220 kJ/mol when determined under similar conditions.¹⁶

If the crystallization is really a two-step procedure, then it should turn out also in DSC tests. The DSC traces in Figure 6 suggest that the exothermic crystallization peaks can be resolved by two overlapping curves in the first approximation. Another important information given by this figure is that the onset of the crystallization process is less dependent on the temperature set. This is adverse with the FBG tests (cf. Figs. 3 and 4), but agrees with the results from normal force measurements (cf. Fig. 5). Considering the FBG, normal force, and DSC results a large scatter can be noticed for the onset of crystallization (cf. Figs. 3–6). First, this has been traced to possible nucleation effects of the discs (rheometer) and pan walls (DSC) opposed to PTFE. Piorkowska et al.¹⁷ pinpointed that such effect may only be at work if the size of the sample is commensurable with that of the crystalline aggregates. This is not the case here. Therefore, we suggest that the onset of crystallization is a stochastic process under such kind of undercooling. Recall that the crystallization of the pCBT occurs $T < 190^\circ\text{C}$ in the related tests, which is below that of the

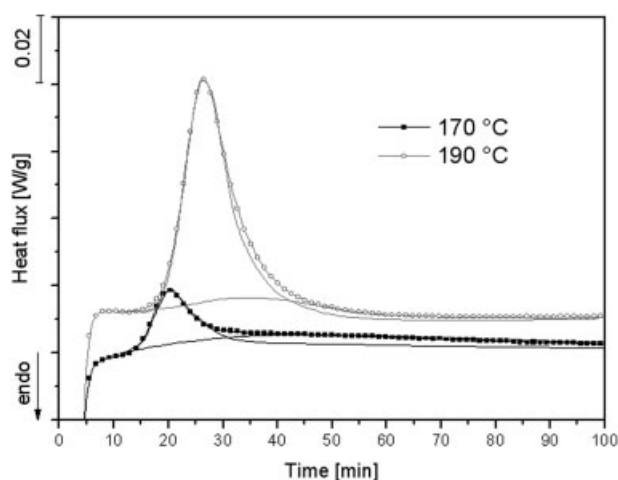


Figure 6 Isothermal DSC traces of CBT samples registered at 170 and 190°C, respectively. Note: the related traces can be resolved by two overlapping curves as indicated schematically.

melting temperature ($T = 225^\circ\text{C}$). A stochastic process involve that crystallization may start before the polymerization is completed, but also when polymerization has been finished. To clarify this issue further investigations are needed.

The next topic that has to be treated is the crystallinity and crystalline structure of the pCBTs. Considering the end of the slow crystallization (section II) in the FBG (Figs. 3 and 4) and normal force measurements (Fig. 5), some differences in respect with the crystalline properties can be expected.

From the DSC traces, registered during isothermal holding, no information can be deduced for the final crystallinity (cf. Fig. 6). This is due to the problem with the baseline assessment owing to the slowly progressing crystallization at lower temperature (cf. DSC trace registered at $T = 170^\circ\text{C}$ in Fig. 6).

Dynamic DSC traces registered during the crystallization from the melt of the pCBTs produced in the FBG tests indicate that the related polymers have similar overall crystallinities (52 and 54% for $T = 170$ and 190°C , respectively). For the melt enthalpy of the 100% crystalline PBT 145 J/g was chosen.¹⁸ Although the overall crystallinity is similar, the crystalline structure of the pCBTs formed at different temperatures, may be different. To check this aspect, the WAXS curves have been analyzed. The related traces in Figure 7 show at the first glance that there is no significant difference between the pCBTs formed at $T = 170$ and 190°C , respectively. The sharp peaks, being in contrast to those of PBT synthesized by polycondensation (also given in Fig. 7), reflect that large, well-developed crystals have been formed.

Figure 7 shows the diffractograms of the two pCBT-samples in comparison with the WAXS spectrum of

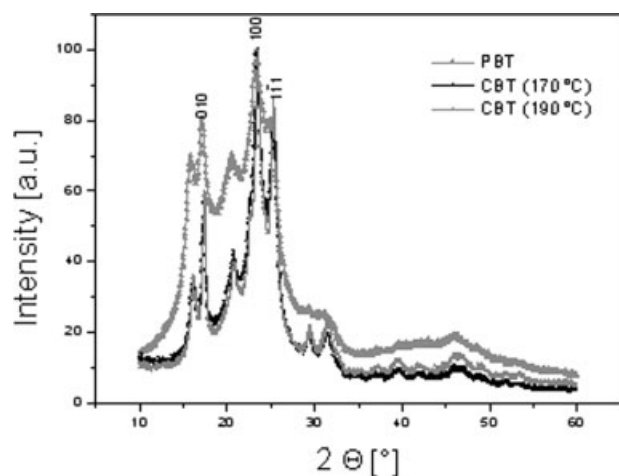


Figure 7 WAXS spectra of pCBTs (from the FBG tests performed at 170 and 190°C, respectively) in comparison with that of a “conventional” PBT (Ultradur B4520 of BASF, Ludwigshafen, Germany).

a “conventional” PBT. The maxima (010), (100), and (111) were described with Gaussian functions, the FWHH was calculated, and the corresponding crystallite sizes (in directions perpendicular to these planes) are summarized in Table I. As expected, regardless the relatively large standard error, the pCBT sample polymerized at $T = 190^{\circ}\text{C}$ possesses somewhat larger crystallites than the pCBT formed at $T = 170^{\circ}\text{C}$. It is noteworthy, that the crystallite sizes determined for the indices (010) and (111) agree fairly with those reported by Parton et al.⁴

When the crystallinity and crystalline fine structures do not differ much from one another, then a similar response is expected from TMA measurements in respect with the thermal expansion characteristics. This was the case, in fact; cf. Figure 8. Note that the TMA measurement served as an independent tool to check the reliability of the FBG technique. Recall that the contraction of the pCBT for the test given in Figure 3 was ca. 140 ppm/°C. The related TMA trace in Figure 8 gives a slightly higher value for the same temperature range (ca. 150 ppm/°C). One can also notice that the TMA curves of the pCBTs, produced at $T = 170$ and 190°C , are very

TABLE I
Apparent Crystallite Size in Direction Perpendicular to the Planes (010), (100), and (111) for the Two Samples, Polymerized and Crystallized at 170 and 190°C, Respectively

Crystallite size (nm)	$T = 170^{\circ}\text{C}$	$T = 190^{\circ}\text{C}$
D(010)	26.8 ± 1.7	30.6 ± 2.9
D(100)	19.9 ± 1.0	25.0 ± 3.0
D(111)	10.4 ± 2.0	12.5 ± 2.7

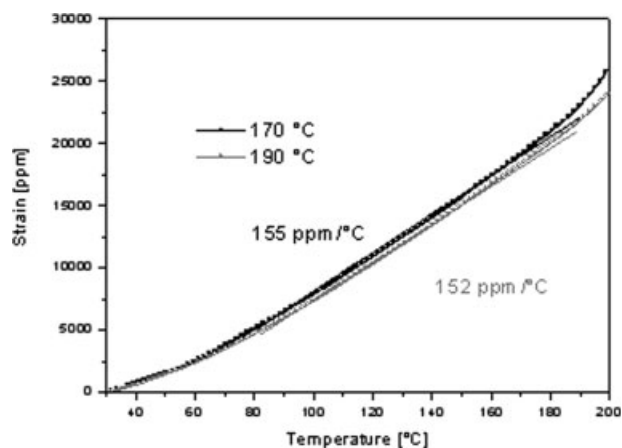


Figure 8 Linear thermal expansion of the pCBTs (from the FBG tests performed at 170 and 190°C, respectively) plotted against the temperature from TMA measurements.

closely matched. This supports the former findings that those parameters which control the thermal behavior (i.e., crystallinity, crystalline fine structure, crystallite size) of the pCBTs, formed in the selected temperature range, are comparable.

CONCLUSION

Based on this work, devoted to study the polymerization and crystallization behaviors of *in situ* polymerized cyclic butylene terephthalate (pCBT) using FBG and normal force measurements, the following conclusions can be drawn:

- The polymerization is highly advanced or even completed before the crystallization starts.
- The FBG and rheological normal force measurements are suitable tools to detect the crystallization-induced shrinkage. It was suggested that the polymerization of CBT does not produce any strain and force signals which was considered as a sign of the entropy-driven polymerization.
- The onset of crystallization is of stochastic nature and the crystallization itself occurs in two steps (primary and secondary). The primary crystallization rate is higher than the secondary one. The rate of the primary crystallization is higher at higher temperature. The activation energy of the primary crystallization was found between 80 and 150 kJ/mol by adopting an Arrhenius equation for the rates derived from FBG and normal force measurements, registered at $T = 170$ and 190°C , respectively. This activation energy, estimated for the crystallization of *in situ* polymerized CBT, is far below that of measured for pCBT crystallizing from the melt.

- The crystalline structure and overall crystallinity were slightly influenced by the selected isothermal conditions ($T = 170$ and 190°C , respectively) as shown by WAXS and other thermal responses (DSC, TMA) of the related pCBTs. The pCBT produced at $T = 190^{\circ}\text{C}$ had somewhat higher crystallinity and larger crystallite sizes than the pCBT formed at $T = 170^{\circ}\text{C}$.

References

1. Brunelle, D. J. In *Modern Polyesters*; Scheirs, J.; Long, T.E., Eds.; Wiley: Chichester, 2003; Chapter 3, p 117.
2. Song, L. N.; Xiao, M.; Shu, D.; Wang, S. J.; Meng, Y. Z. *J Mater Sci* 2007, 42, 1156.
3. Tripathy, A. R.; MacKnight, W. J.; Kukureka, S. N. *Macromolecules* 2004, 37, 6793.
4. Parton, H.; Baets, J.; Lipnik, P.; Goderis, B.; Devaux, J.; Verpoest, I. *Polymer* 2005, 46, 9871.
5. Tripathy, A. R.; Elmoumni, A.; Winter, H. H.; MacKnight, W. J. *Macromolecules* 2005, 38, 709.
6. Parton, H.; Verpoest, I. *Polym Compos* 2005, 26, 60.
7. Mohd Ishak, Z. A.; Gatos, K. G.; Karger-Kocsis, J. *Polym Eng Sci* 2006, 46, 743.
8. Mohd Ishak, Z. A.; Leong, Y. W.; Steeg, M.; Karger-Kocsis, J. *Compos Sci Technol* 2007, 67, 390.
9. Mohd Ishak, Z. A.; Shang, P. P.; Karger-Kocsis, J. *J Thermal Anal Calorim* 2006, 84, 637.
10. Karger-Kocsis, J.; Shang, P. P.; Mohd Ishak, Z. A.; Rösch, M. *eXPRESS Polym Lett* 2007, 1, 60.
11. Harsch, M.; Karger-Kocsis, J.; Herzog, F. *Macromol Mater Eng* 2007, 292, 474.
12. Harsch, M.; Karger-Kocsis, J.; Herzog, F. *J Appl Polym Sci* 2008, 107, 719.
13. Harsch, M.; Karger-Kocsis, J.; Herzog, F. *eXPRESS Polym Lett* 2007, 1, 226.
14. Yashiro, S.; Okabe, T.; Takeda, N. *Compos Sci Technol* 2007, 67, 286.
15. Othonos, A.; Kalli, K. *Fiber Bragg Gratings*; Artech House: Boston, 1999; p 95.
16. Lehmann, B.; Karger-Kocsis, J. *J Thermal Anal Coloum*, submitted.
17. Piorkowska, E.; Galeski, A.; Haudin, J.-M. *Progr Polym Sci* 2006, 31, 549.
18. ATHAS database. Available at <http://web.utk.edu/~athas/databank/>. Accessed on May, 2007.